Soil & Tillage Research 266 (2027) 107485

Contents lists available at ScienceDirect

Soil & Tillage Research

journal homepage: www.elsevier.com/locate/still

Quantifying soil aggregate hierarchy through energy-based dispersion modelling in contrasting soil types and land uses

Rodrigo Lima da Motta Junior [a,*], Steffen A. Schweizer [b], Bernardo Amorim da Silva [c], Franziska Bucka [d], Thiago M. Inagaki [e], Noelia Garcia-Franco [b,f], Evelin Pihlap [g,h], Edson Marcio Mattiello [a], Ingrid Kögel-Knabner [b,i], Pedro P. de C. Teixeira [j]

[a] Departamento de Solos, Universidade Federal de Viçosa, Campus Universitário s/n, Viçosa, Minas Gerais, 36.570-900, Brazil
[b] Chair of Soil Science, Technical University of Munich, Emil-Ramann-Straße 2, Freising, 85354, Germany
[c] Embrapa Hortaliças, Rodovia BR 060 Km 9, Samambaia Norte, Brasília - DF, 70351-970, Brazil
[d] Soil Geography and Ecosystem Research, Institute of Physical Geography, Goethe University Frankfurt, Altenhöferallee 1, Frankfurt am Main, 60438, Germany
[e] Norwegian Institute of Bioeconomy Research (NIBIO), Department of Biogeochemistry and Soil Quality, Høgskoleveien 7, Ås, 1430, Norway
[f] Division of Plant-Production Systems, Agroscope, Nyon, Switzerland
[g] Soil Science, Centre of Estonian Rural Research and Knowledge, J. Aamisepa 1, Jõgeva Township, Jõgeva County, 48309, Estonia
[h] Institute of Ecology and Earth Sciences, University of Tartu, Vanemuise 46, Tartu, 51003, Estonia
[i] Institute for Advanced Study, Technical University of Munich, Lichtenbergstraße 2a, Garching, 85748, Germany
[j] Karlsruhe Institute of Technology (KIT), Institute of Geography and Geoecology, Reinhard-Baumeister-Platz 1, Karlsruhe, 76131, Germany

ARTICLE INFO

Keywords:
Soil aggregation
Ultrasonic dispersion
Tillage management
Binding agents

ABSTRACT

Aggregate hierarchy, the organization by which microaggregates form progressively larger, structurally distinct macroaggregates, is central to soil stability, governing resistance to erosion and response to disturbance. However, the mechanisms and extent of hierarchical breakdown remain poorly quantified across different soil types and land management. In this study, we addressed this gap by evaluating the stepwise breakdown of soil structure into aggregates, driven by incremental sonication energy, across a range of soils differing in mineral composition and management practices. By applying a quantitative modelling framework, we derived three key parameters: the disruption constant (k_1), reflecting the rate of aggregate breakdown; the dispersion constant (k_2), which describes particle release; and the critical energy threshold (E_{crit}), which denotes the transition point between aggregate disruption and full particle dispersion. These parameters were used to evaluate the degree of hierarchy in aggregate breakdown, whereby higher k_1/k_2 ratios signal a pronounced stepwise (hierarchical) disintegration, and ratios near unity indicate direct dispersion into clay-sized particles. Our results indicated that soils enriched in 2:1 phyllosilicate clay minerals, such as Luvisols, exhibited markedly higher k_1/k_2 ratios in larger aggregates, demonstrating a structured, multi-step breakdown process. In contrast, oxide-rich soils like Ferralsols and Andosols typically lacked such hierarchy, dispersing rapidly into smaller fractions, which is consistent with a stronger role of mineral-mineral binding relative to organic-mediated aggregation. In the studied Luvisols, direct seeding was associated with higher stability (higher E_{crit}) and a greater degree of hierarchy than conventional tillage, emphasizing the synergistic effects of organic matter input and reduced disturbance on soil structural integrity. These findings highlight the mechanistic roles of distinct pedogenic groups and management practices in controlling aggregate hierarchy and stability. Our study shows that sonication-derived indicators can differentiate not only distinct pedogenic groups but also soil management. These indices can be further developed to provide a quantitative insight into the structural organization that underpins water retention, erosion resistance, and other soil functions critical for conservation.

* Corresponding author.
E-mail address: rodrigo.motta@ufv.br (R.L. da Motta Junior).

https://doi.org/10.1016/j.still.2026.107485
Received 22 May 2026; Received in revised form 9 September 2026; Accepted 10 September 2026
Available online 14 September 2026

The Article Processing Charge for the publication of this research was funded by the Coordenação de Aperfeiçoamento de Pessoal de Nível Superior - Brasil (CAPES) (ROR identifier: 00x0ma614).

1. Introduction

Soil structure underpins essential ecosystem functions, regulating water retention, root development, carbon sequestration, and biotic activity, and thereby directly shaping plant productivity and resilience to environmental stress (Bronick and Lal, 2005). The most widely accepted model for describing how soil components are organized across scales is the aggregate hierarchy model (Jarvis et al., 2012). According to this model, aggregates result from the physical and chemical interactions of binding agents such as organic matter, clay minerals, and oxide surfaces, which together give rise to a hierarchical and nested organization: microaggregates (<53 μm) serve as the fundamental units embedded within larger macroaggregates (>250 μm) (Oades, 1984; Six et al., 2004; Totsche et al., 2018). Aggregate stability is determined by the interplay between organic binding (via polysaccharides and microbial exudates), mineral cohesion (predominantly by clay minerals), and cementation by pedogenic oxides and calcium carbonates, with the relative roles of these agents varying among soil types and environmental settings (Tisdall and Oades, 1982). The aggregate hierarchy concept is foundational for understanding how soils resist disturbance and retain physical structure, with hierarchical organization linked to resilience against erosion, improved water and nutrient cycling, and broader ecosystem functioning through its effects on infiltration, drainage, plant productivity, and microbial activity (Fatichi et al., 2020). Traditionally, aggregate hierarchy has been viewed as an intrinsic property controlled by mineralogical composition (Kögel-Knabner and Amelung, 2021; Oades and Waters, 1991; Six et al., 2004; Totsche et al., 2018). However, it remains unclear whether hierarchy is a static feature or instead reflects current soil conditions, such as organic matter status (Dexter et al., 2008) and recent management (Lal, 2015).

One of the first attempts to test soil aggregate hierarchy was provided by Oades and Waters (1991) who articulated the hierarchical fragmentation hypothesis. This hypothesis describes that soils with aggregate hierarchy should exhibit a stepwise breakdown of soil structure, wherein larger, loosely bound macroaggregates are sequentially fragmented into microaggregates before dispersion into smaller fractions. Later, new evidence revealed that complete dispersion into true primary particles is rarely achieved in soil systems, as even under strong dispersion energy, persistent associations between mineral particles and organic or inorganic binding agents remain (Chenu and Plante, 2006; Christensen, 2001). This was observed in soils where aggregate stability is controlled by soil organic matter, but not in oxide-rich soils. In this way, the aggregate hierarchy could not be extended to all soil types. More recently, this notion has been challenged by several studies that investigated soil aggregation using microscopy techniques (Asano and Wagai, 2014; Vrdoljak and Sposito, 2002). Although these studies identified the binding agents responsible for the aggregation, especially in the sub-micron range, they were unable to test for the hierarchical fragmentation hypothesis as described by Oades and Waters (1991), because they did not test for the stepwise breakdown of aggregates.

One major limitation of the approach used by Oades and Waters (1991) to test the hierarchical fragmentation hypothesis is that it relied on only a few energy-disruption levels. Building on this concept, Field et al. (2006) developed a modelling approach based on full breakdown curves to quantify the rates and energy thresholds of aggregate liberation and subsequent clay dispersion. This approach enables the resolution of hierarchical levels through continuous relationships between applied energy and aggregate disruption. To date, however, this modeling framework has been applied mainly to a narrow set of soils, and its performance in soils of different pedogenic groups, with contrasting mineral composition, parent materials, and management histories, has not been systematically evaluated. Applying such energy-based, hierarchy-sensitive indices across a broader soil set offers an opportunity to move beyond binary stability classes and to test whether differences in binding agents and management regimes indeed manifest as measurable differences in aggregate hierarchy and stability. While numerous empirical approaches exist for assessing aggregate stability, such as slaking, wet sieving, or ultrasonic dispersion, a major limitation is that they typically use a single, arbitrary energy level, thereby classifying aggregates only as “stable” or “unstable” at that specific intensity. As a result, these methods provide limited insight into how aggregates respond across an energy continuum and are poorly aligned with the concept of hierarchy as a gradational property. A further critical gap is the influence of anthropogenic factors, such as long-term tillage or reclamation practices, which modulate aggregate hierarchy by altering the abundance, composition, and distribution of binding agents.

This study addresses two major knowledge gaps: (i) whether the degree of hierarchical aggregation differs among soils from distinct pedogenic groups, and (ii) the extent to which soil management can modify this hierarchical organization. To this end, we studied soils from contrasting pedogenic groups and managements: Ferralsols and Andosols (characterized by microaggregate-dominated oxide cementation), Luvisols (featuring variable 2:1 clay and organic matter associations under different tillage regimes), a Calcaric Regosol (reclamation/disturbance) in the initial state of formation, and a C-rich Phaeozem. By systematically modelling aggregate fraction responses to stepwise ultrasonic energy, we aim to determine whether pedogenic groups and management-related differences manifest in measurable variations in aggregate hierarchy.

2. Material and methods

2.1. Soil samples and sample preparation

Soil samples were collected at the A horizon across sites representing contrasting soil types and land management systems. Two Cambic Luvisols (IUSS Working Group, 2015) samples were obtained from the Puch long-term experiment in south-east Germany: one under direct seeding (LDS) and one under conventional tillage management (LCT), both presenting similar soil texture. In addition, two samples were collected from the Garzweiler open-mining area (Germany): a Calcaric Regosol (IUSS Working Group, 2015) from a 24-year-old reclamation site (CRR, 51°5′ N, 6°28′ E, post-mining fields, 5 km west of Grevenbroich) and a Luvisol from an adjacent undisturbed reference area (LRS, 51∘5′N, 6∘28′E, approximately 40 km west of Cologne, Germany) (IUSS Working Group, 2015). Additional soils were obtained from distinct pedogenic environments: a Ferralsol (FER, 21°01’37” S 42°34’12” W, Vargem Alegre, Brazil) (IUSS Working Group, 2015), an Andosol (AND, 20° 3′35"N, 155°43'56"O) from Hawaii, United States, and a Phaeozem (PHA, 11.03° E, 47.57° N, Graswang at an altitude of 860 m above sea level) (IUSS Working Group, 2015). The selected soils were chosen to represent a broad range of pedological environments, mineralogical compositions, and land-use conditions to test the applicability of the proposed energy-based framework across contrasting soil systems. Specifically, the dataset encompasses soils representing the major aggregate stabilization mechanisms described in the literature, including phyllosilicate-dominated soils, oxide-rich tropical soils, and Andosols characterized by short-range-order minerals, as well as contrasting management systems to evaluate the sensitivity of the proposed framework to land-use-induced changes in aggregate hierarchy. The key physicochemical properties of each site are summarized in Table 1.

2.2. Sample sonication

Air-dried samples were gently disaggregated and sieved to obtain a fraction smaller than 5 mm. 3 g of soil was immersed in 30 mL of deionized water in glass containers (27 mm internal diameter, 96 mm height) for sonication. The containers were placed in an ice-water bath during sonication to prevent overheating. Because the objective was to examine aggregation and disruption processes governed by distinct

Table 1
Key physicochemical properties for each of the samples.

Soil type	Bulk density (g cm^{-c})	Particle density (g cm^{-c})	Clay (g kg^{-a})	Silt (g kg^{-a})	Sand (g kg^{-a})	FeO_d (mg g^{-a})	AlO_d (mg g^{-a})	TN (%)	SOC (%)	TC (%)
1. Luvisol, conventional tillage	0.921	2.67	-	-	-	-	-	0.13	1.23	-
2. Luvisol, direct seeding	1.061	2.65	388[b]	460[b]	1522	142[b]	-	0.18	1.76	-
3. Andosol[c]	-	2.42	-	-	-	81.71	29.30	0.87	8.9	-
4. Ferralsol[d]	1.13	2.69	660	90	250	-	-	0.21	3.24	-
5. Calcaric Regosol (24-year reclamation site)[e]	-	2.73	318	653	29	-	-	0.05	0.57	1.4
6. Luvisol (reclamations reference site)[e]	-	2.61	-	-	-	-	-	0.09	0.97	0.97
7. Phaeozem[f]	0.5	2.05	615	353	32	19.9	3	1.9	17.44	-

[a] Data by Krauss et al. (2022);
[b] data by Wu et al. (2022);
[c] data by Teixeira et al. (2024);
[d] data by Inagaki et al. (2020);
[e] data by Pihlap et al. (2021);
[f] data by Garcia-Franco et al. (2021). FeOd: dithionite-extracted iron; AlOd: dithionite-extracted aluminum; TN: total nitrogen; SOC: soil organic carbon; TC: total carbon. "-" indicates data not available.

binding agents, no pre-treatment was applied.

Sonication was performed using a probe-type ultrasonic device (Sonopuls HD2200, Bandelin electronic GmbH, Germany) with adjustable power output. Ultrasound was applied via a cylindrical probe (13 mm in length, 20 kHz oscillation frequency) inserted 5 cm into the suspension.

Energy input (E) was calculated according to North (1976), with probe calibration accounting for the total energy delivered, including thermal and conductive losses. Sonication times ranged from a few seconds to approximately 28 min, depending on the target energy level (Table 2). Sonication periods exceeding 6 min were avoided to prevent overheating. Each soil type was analysed in triplicate at all applied energy levels (Table 2). The ultrasonic energy gradients were defined individually for each soil because aggregate stability and dispersion behavior vary substantially among soil types. Preliminary tests were conducted to identify the minimum and maximum energy levels required to characterize the complete aggregate liberation and clay dispersion curve of each soil. In addition, the selected energy gradients ensured that sufficient material smaller than 53 μm was produced to exceed the detection limit required for reliable particle-size determination using the Sedigraph. Consequently, although the absolute energy ranges differed among soils, each gradient was designed to adequately capture the dispersion behavior of the respective soil. Although the use of soil-specific energy gradients allowed complete dispersion curves to be captured for each soil, comparisons of the fitted model parameters among soils should be interpreted with caution, because these parameters were derived over different absolute energy ranges.

Table 2
Energy input on each soil sample.

Soil type	Applied energy						
	J/mL						
Luvisol (conventional tillage)	0	10	30	60	120	260	
1. Luvisol (direct seeding)	0	10	30	60	120	260	
1. Andosol	0	120	260	460	800	1200	1800
2. Ferralsol	0	120	260	460	800	1200	1800
3. Calcaric Regosol (24 years reclamation site)	0	10	30	60	120	260	
4. Luvisol (reclamation reference site)	0	10	30	60	120	260	
5. Phaeozem	0	260	460	800	1200	1800	2400

2.3. Aggregate and particle size distribution

The effect of applied ultrasonic energy on aggregate breakdown was assessed by measuring aggregate and particle size distributions at increasing energy levels. After sonication, each suspension underwent sequential fractionation. First, a gentle wet-sieving procedure separated aggregates into > 250 μm and 250–53 μm fractions. Material retained on each sieve was transferred to beakers, oven-dried at 105°C for 24 h, and weighed.

The remaining suspension (<53 μm) was subjected to particle size analysis using a Sedigraph III Plus (Micrometrics GmbH, Germany), which determines particle size distribution via gravitational sedimentation coupled with X-ray absorption. Particle size classification followed Stokes' law (Gee and Or, 2002), resulting in four finer fractions: 53–20 μm, 20–6.3 μm, 6.3–2 μm, and < 2 μm. The < 53 μm fractions were analysed using the SediGraph, while coarse fractions (>53 μm) were quantified by sieving. Particle size distribution was expressed as a percentage of the initial sample's dry mass (normalized to 100%). For the sieved fractions (>250 μm and 250–53 μm), mass percentages were calculated directly from the retained dry weight. For the < 53 μm fraction, its mass was calculated by subtracting the combined mass of the coarser fractions from the total initial sample weight. Subsequently, the proportional contribution of each fine-size fraction (53–20, 20–6.3, 6.3–2, and <2 μm) was determined using the SediGraph.Fig. 1

2.4. Aggregate disruption and dispersion modelling

To quantify the relationship between applied ultrasonic energy and aggregate dispersion, curve fitting was performed as described in Field and Minasny (1999). Three characteristic curves were derived:

2.4.1. Soil dispersion characteristic curve (SDCC)

The SDCC describes the cumulative release of clay-sized particles (<2 μm) as a function of increasing energy input and follows an exponential saturation model:

$$SDCC = A_0[(1 - \exp(-k_2)E)]$$

where A_0 represents the total dispersible clay content (%), defined as the mass of clay-sized particles released at the maximum applied energy level; k_2 is the fitted dispersion rate constant; and E is the applied energy (J mL^{-1}).

2.4.2. Aggregate disruption characteristic curve (ADCC)

The ADCC describes the reduction in macro and microaggregate fractions (>250 μm, >53 μm, >20 μm, and > 6.3 μm) with increasing energy. The ADCC follows a negative exponential model:

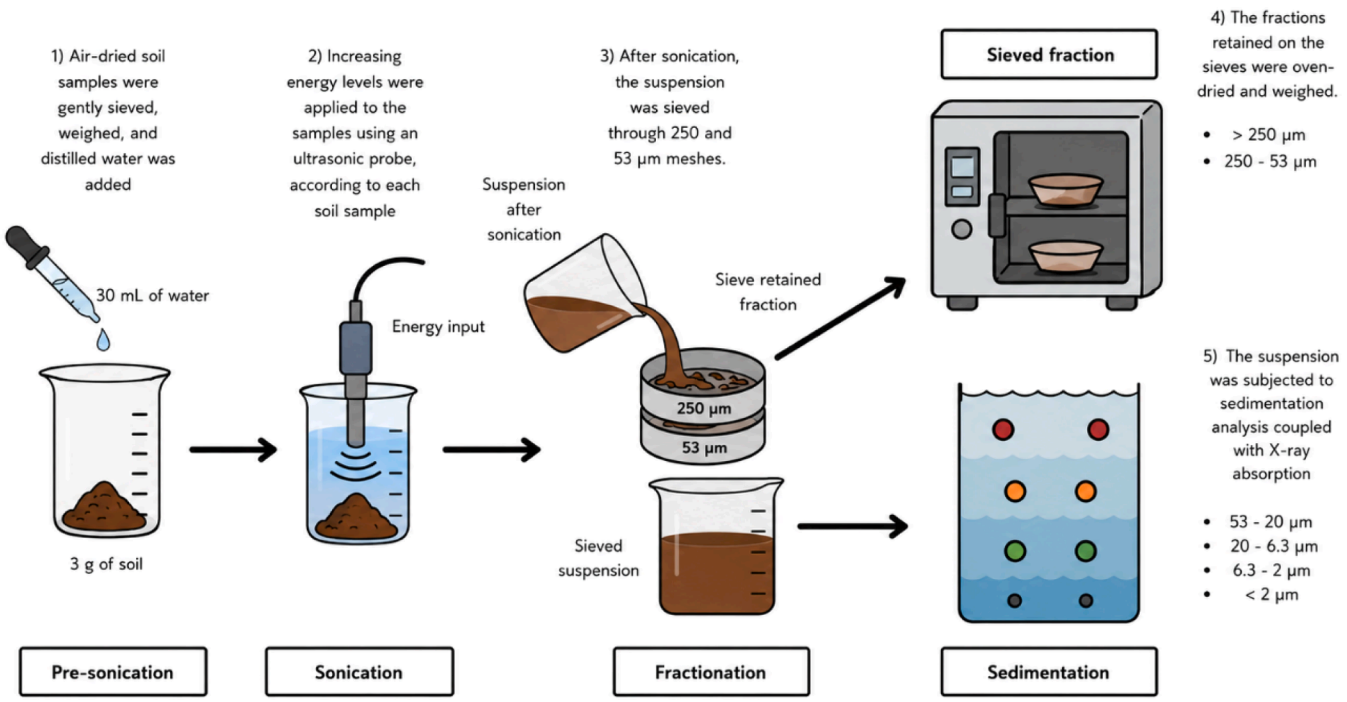

Fig. 1. Methodology scheme of sample preparation, sonication and fractionation.

$$ADCC = A_0\exp(-k_1E) + C_1$$

k_1 is the fitted disruption rate constant, and C_1 represents the residual undisturbed fraction remaining at the highest applied energy level (mineral particles).

2.4.3. Aggregate liberation and dispersion curve (ALDC)

The ALDC integrates both dispersion and disruption phases, capturing the sequential breakdown of aggregates into smaller particles and their subsequent dispersion. The ALDC is modeled as a first-order consecutive reaction:$ALDC = -A_0[(\exp(-k_1)E) - \exp(-k_2)E)] + C_2$

where C_2 accounts for the intermediate fraction (250–2 µm, 53–2 µm, 20–2 µm, 6.3–2 µm), expressing the balance between aggregate disruption and post-liberation dispersion.

To adjust the equations and estimate the disruption and dispersion constants (k_1 and k_2), the parameters A_0, C_1, and C_2 were defined as start values based on the proportion of each fraction (clay, intermediate, and larger) measured at the highest applied energy level for each soil.

2.4.4. Critical energy (E_{crit})

The critical energy (E_{crit}) was defined as the energy at which the rate of aggregate liberation equals the rate of dispersion. Prior to E_{crit}, aggregate breakdown dominates; beyond E_{crit}, dispersion into clay-sized particles is the dominant process. Because E_{crit} is derived from the intersection of two exponential functions, Equation 4 is only defined when $k_1 \neq k_2$.$Ecrit = \frac{\ln(\frac{k_2}{k_1})}{k_2 - k_1}$

The k_1/k_2 ratio was used to assess the balance between aggregate disruption and particle dispersion, providing a quantitative measure of aggregate hierarchy. To further explore hierarchical structuring, a classification range was established based on the k_1/k_2 ratio:

This classification quantifies the relative dominance of disruption versus dispersion, with higher ratios indicating stronger intra-aggregate bonding relative to inter-aggregate structuring and a more stepwise breakdown process. Fig. 2 illustrates the effect of varying k_1/k_2 ratios on the ALDC, where increased hierarchy (higher k_1/k_2) leads to more distinct transitions between the disruption and dispersion phases. In the simulation shown, all parameters except k_2 are held constant to isolate the effect of hierarchy on curve morphology.

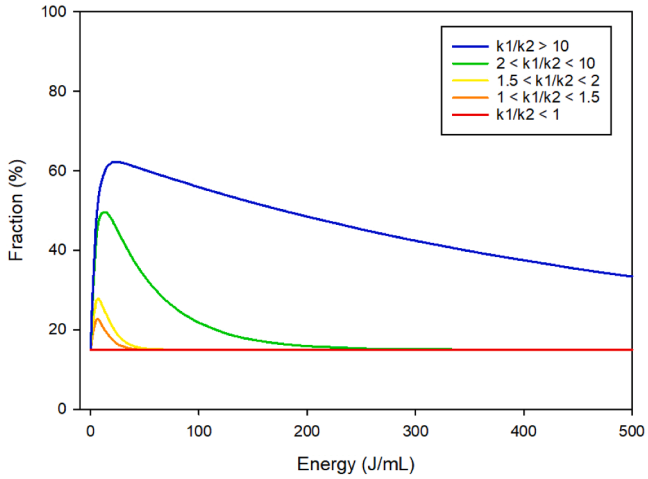

Fig. 2. Simulated aggregate liberation and dispersion curves illustrating the conceptual effect of varying k_1/k_2 ratios on curve shape. The disruption rate (k_1) was held constant while only the dispersion rate (k_2) was varied. Higher k_1/k_2 ratios produce a longer transition phase (tail), reflecting a more gradual, stepwise aggregate breakdown before clay dispersion and, consequently, a greater degree of aggregate hierarchy. The figure is intended solely as a conceptual illustration and does not represent experimental data.

To investigate aggregate breakdown and dispersion patterns within the same soil, we defined discrete particle-size intervals within the microaggregate fractions (0–2, 2–6.3, 6.3–20, 20–53, 53–250 µm). The mass within each interval was calculated as the difference between successive cumulative size classes, enabling quantification of mass transfer across size fractions during dispersion (Field et al., 2006). Nonlinear regression was performed using the Nonlinear Least Squares function in RStudio (R Core Team, 2026), with minpack.lm, and results were visualized using OriginPro 2025. Accordingly, as the parameters were derived from nonlinear model fitting, comparisons among soils and

size fractions were based on the descriptive interpretation of fitted model behavior.

3. Results

3.1. Aggregate hierarchy

Aggregate Liberation and Dispersion Curves (ALDCs) for four microaggregate size fractions (2–6.3 μm, 2–20 μm, 2–53 μm, and 2–250 μm) were generated for the Luvisols, Calcaric Regosol, Ferralsol, Andosol, and Phaeozem (Fig. 3). Across all soils except the Phaeozem, the k_1/k_2 ratio decreased with decreasing aggregate size, indicating that aggregate hierarchy weakened towards finer fractions and that hierarchical organization is primarily expressed in larger microaggregates.

In the Luvisols, the highest degree of hierarchy was observed in the largest microaggregate fraction (2–250 μm; Fig. 4), where k_1/k_2 ratios of 7.1 (conventional tillage) and 9.8 (direct seeding) denote an intermediate hierarchical level (Table 3). As aggregate size diminished, k_1/k_2 declined and differences between management systems- narrowed, but hierarchy persisted in the finest fraction (2–6.3 μm), with k_1/k_2 values of 2.4 (conventional tillage) and 2.0 (direct seeding), denoting a reduced yet still hierarchical organization. Notably, while the disruption rate constant (k_1) was comparable between management systems, the dispersion rate constant (k_2) was more than 20% lower under direct seeding, indicating that reduced disturbance primarily acts by decreasing dispersion rates at the microaggregate scale rather than by altering the rate of aggregate disruption.

Similar hierarchical patterns were observed in the Calcaric Regosol and the Luvisol at the mining area. Both soils exhibited maximum k_1/k_2 ratios in the 2–250 μm fraction (14.15 and 9.01, respectively), indicative of high to intermediate aggregate hierarchy in the coarsest microaggregates. In both cases, k_1/k_2 decreased to 1.26–1.67 in the finer fractions, suggesting that hierarchical structuring progressively weakens at smaller aggregate sizes.

In contrast, the Ferralsol showed k_1/k_2 ratios close to unity across all size fractions, consistent with an absence of hierarchical aggregation and a more direct dispersion process into clay-sized particles. The Andosol expressed a pronounced hierarchy only in the 2–250 μm fraction ($k_1/k_2 = 33.31$), whereas the hierarchical trend largely dissipated for smaller aggregate classes. Distinct from the other soils, the Phaeozem showed a contrasting pattern: k_1/k_2 values increased with decreasing aggregate size, with the highest ratio (5.46) observed in the 2–6.3μm fraction. This indicates that hierarchical organization was not expressed in the larger fractions of this soil.

3.2. Critical energy

Critical energy values provided complementary information on the resistance of each size fraction to dispersion across soils. Luvisols under conventional tillage consistently exhibited lower E_{crit} than Luvisols under direct seeding in all fractions, indicating greater resistance to dispersion under reduced disturbance. This difference was most pronounced in the 2–6.3 μm fraction, where E_{crit} reached 24.89 J/mL for direct seeding and 14.25 J/mL for tilled soil.

At the mining sites, E_{crit} ranged from 6.28 J/mL to 27.71 J/mL in the Calcaric Regosol from the reclamation area and from 10.67 J/mL to 29.71 J/mL in the Luvisol from the mining area. In both soils, the highest E_{crit} values occurred in the 2–6.3 μm fraction, suggesting that the finer operational fractions required more energy to reach the transition between disruption and dispersion in both reclaimed and reference systems.

For the Ferralsol and the Andosol, E_{crit} increased in smaller fractions but with distinct magnitudes. In the 2–6.3 μm fraction, the Andosol required substantially more energy to disperse (655 J/mL) than the Ferralsol (459 J/mL), whereas in the 2–250 μm fraction the Ferralsol (329 J/mL) was more resistant than the Andosol (65 J/mL).

The Phaeozem displayed the opposite pattern, with larger fractions having the highest E_{crit} values (2146.14 J/mL for 2–250 μm and 2288.39 J/mL for 2–53 μm), while smaller fractions exhibited lower E_{crit}, indicating that larger aggregates in this C-rich soil are highly resistant to dispersion whereas smaller aggregates are comparatively more susceptible.

4. Discussion

4.1. Aggregate hierarchy across soils from distinct pedogenic groups

The results demonstrate that hierarchical aggregation can be quantitatively characterized across soils using the k_1/k_2 ratio, which captures differences in aggregate disruption and dispersion patterns. This provides a measurable framework for evaluating the degree of hierarchical organization in soils, as predicted by the hierarchical fragmentation hypothesis. However, while this hypothesis is supported for most soils tested, it does not adequately describe the behavior observed in the Phaeozem. Unlike previous reports, which established the existence of hierarchical aggregation (Six et al., 2004; Tisdall and Oades, 1982), our findings show that the degree and strength of hierarchy vary systematically among soils from distinct pedogenic groups. In this sense, the energy-resolved k_1/k_2 framework extends classic aggregate hierarchy models by quantifying hierarchy across contrasting mineralogical settings and management regimes, rather than treating hierarchy as a binary property. To our knowledge, this relationship has not previously been quantified at this level of resolution across diverse soils and management practices, thereby providing a mechanistic basis for comparing hierarchical fragmentation among soil types.

Our results reveal that the Luvisols, commonly associated with 2:1 phyllosilicate minerals (IUSS Working Group, 2015), exhibited intermediate aggregate hierarchy, especially in the 2–250 μm size class (Table 3, Fig. 4). This pronounced stepwise breakdown supports prior hypotheses, and the empirical resolution across size fractions and tillage systems suggests an association between management-related organic inputs and the maintenance of aggregate hierarchy (Poeplau et al., 2020). Ferralsol and Andosol samples behaved distinctly from the Luvisols from the Puch long-term experiment (LDS and LCT), consistent with previous studies that showed a lack of hierarchy in these soils (Oades and Waters, 1991). Notably, the Andosol displayed hierarchy only in the largest fraction, suggesting a conditional role for organic carbon in microaggregate clustering even in highly weathered matrices. At the microscale, the apparent lack of hierarchical organization may reflect the high stability of mineral associations, driven by cementation involving both crystalline and amorphous Fe and Al oxides (Breure et al., 2026), as well as potential clay re-aggregation during the experimental procedure in Andosols (Inagaki et al., 2020). In this context, these data are consistent with the notion that aggregate formation in oxide-rich tropical soils relies predominantly on mineral-mineral interaction, limiting the development of multi-level aggregate frameworks (Emerson and Greenland, 1990). The E_{crit} denotes the energy level at which aggregate disruption and dispersion occur at equal rates, providing a measurement of the stability of a given size fraction. Microaggregate stability was most pronounced in Ferralsols and Andosols, aligning with established concepts of oxide-driven microaggregate cementation (Denef et al., 2002; Oades, 1989). Conversely, in the Phaeozem, which develops on calcareous and dolomitic parent material, characterized by high carbonate content, the model did not adequately explain aggregation behavior. Indeed, the low ALDC model fit for the 2–250 and 2–53 μm fractions ($R^2 = 0.26$ for both, Table 4) indicates that the framework may not adequately capture the dispersion behavior of the larger Phaeozem fractions. Consequently, the fitted parameters for these fractions, including E_{crit}, should be interpreted with caution. The parent material, primarily composed of limestone and dolomite, contains significant amounts of Mg^{2+} and Ca^{2+}, which Garcia-Franco et al. (2021) showed can influence the strength of soil aggregation. Although

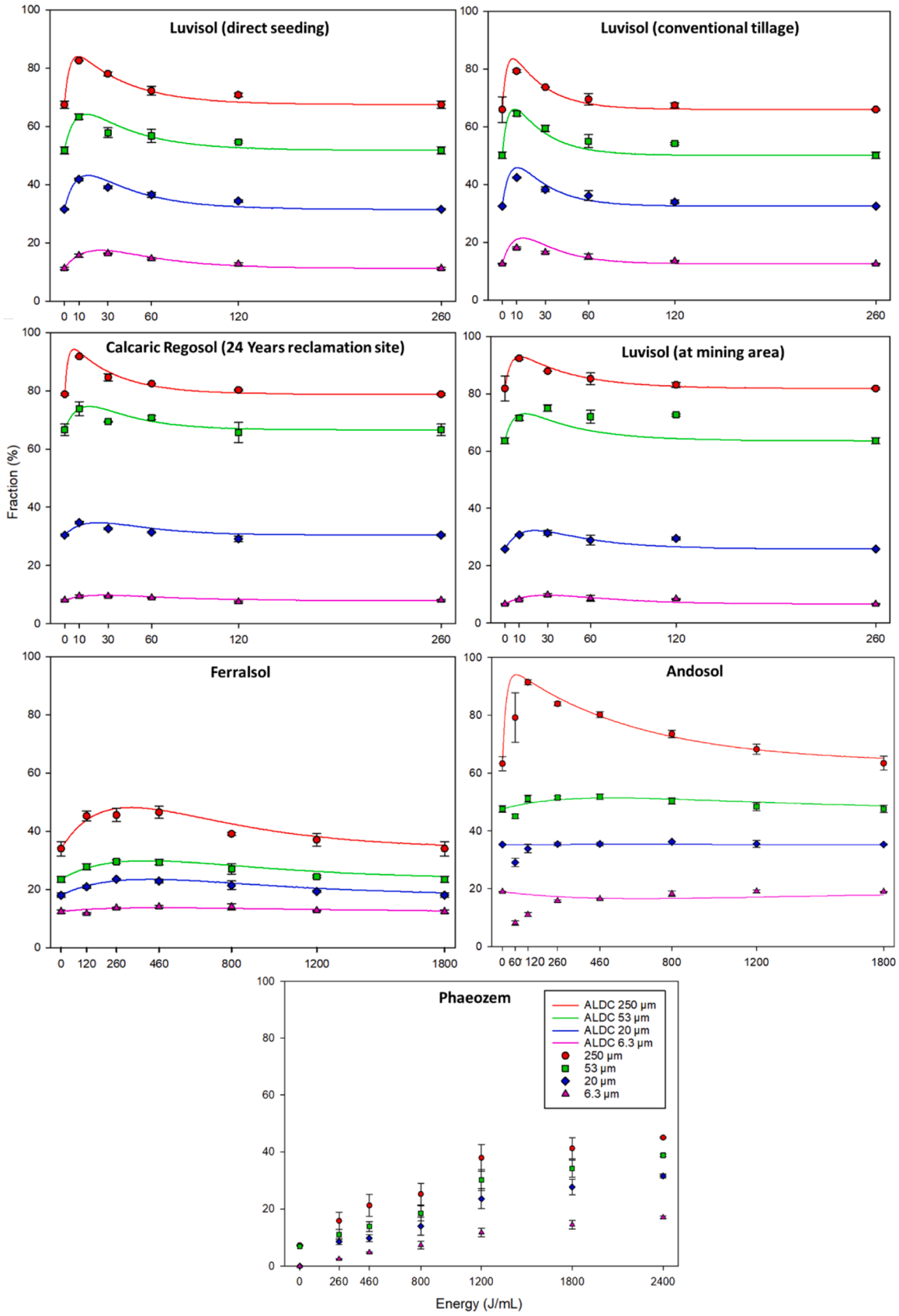

Fig. 3. Relationship between the total energy applied and proportion of material in the Aggregate Liberation and Dispersion Curves (ALDCs) that shows the 2–6.3 (clay- and fine silt-sized particles), 2–20 (clay- and silt-sized particles), 2–53 (small microaggregates), and 2–250 (large microaggregates) µm fractions for the Ferralsol, Andosol, Luvisol till, Luvisol direct seeding, Luvisol at the mining area), Calcaric Regosol (24 years reclamation site), and Phaeozem.

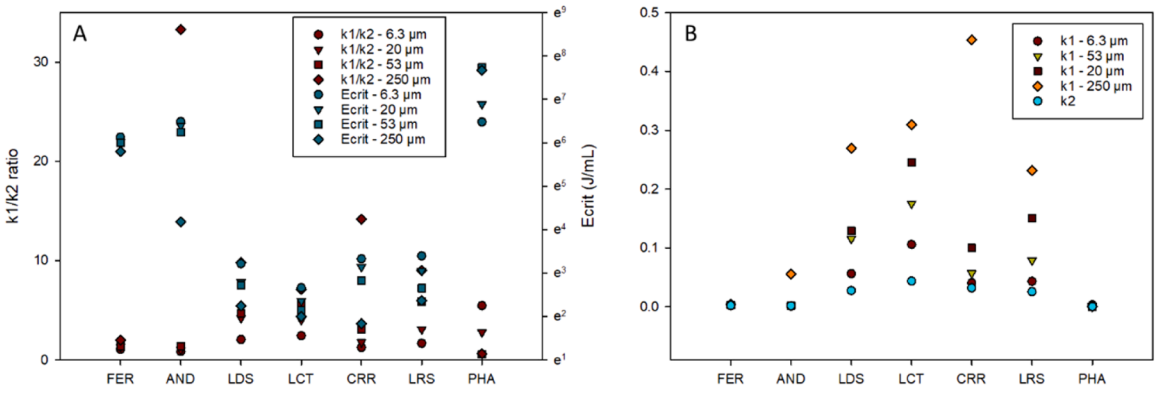

Fig. 4. Variation of k_1/k_2 ratio, critical energy (E_{crit}) (A), and rate constants (k_1 and k_2) (B) across soil types and aggregate size fractions.

Table 3
Proposed classification of aggregate hierarchy based on the relative rates of aggregate disruption (k_1) and particle dispersion (k_2).

k_1/k_2	Hierarchy classification
< 1	No hierarchy: The rate of aggregate disruption is lower than the rate of clay-sized particle dispersion.
$1 < k_1/k_2 \leq 2$	Low hierarchy: The rate of aggregate disruption is up to two times higher than the rate of clay-sized particle dispersion.
$2 < k_1/k_2 \leq 10$	Intermediate hierarchy: The rate of aggregate disruption is two to ten times higher than the rate of clay-sized particle dispersion.
> 10	High hierarchy: The rate of aggregate disruption is more than ten times higher than the clay-sized particle dispersion.

the high fitted Ecrit values in the coarser fractions could be compatible with greater resistance of carbonate-cemented aggregates to disruption, the low model fit prevents a robust interpretation of these values. However, we did not directly quantify carbonate distribution within aggregates, so this interpretation should be regarded as a mechanistic hypothesis informed by known processes rather than a direct confirmation of carbonate effects in our samples. Taken together, differences in E_{crit} across size fractions and soil types provide a useful bridge between classic hierarchy concepts and the specific mineralogical controls (oxides, carbonates, phyllosilicates) operating in each pedogenic group.

4.2. Hierarchy degree as indices for soil management and reclamation

Our comparison of long-term management and reclamation provides evidence that in the studied Luvisol system, conservation management was associated with greater aggregate hierarchy and resistance to dispersion. In the direct seeding Luvisol (LDS), higher E_{crit} values and a comparatively greater degree of hierarchy were observed relative to conventionally tilled soils (LCT; Table 3). These differences correspond with higher soil organic carbon contents measured in the LDS system (1.76%, Table 1), supporting the idea that SOC input is a critical factor in stabilizing aggregates and promoting hierarchical organization. Moreover, it should be kept in mind that mechanical disturbance during plowing disrupts aggregates and contributes to a reduction in the degree of hierarchy, so both increased SOC and reduced physical disturbance act together to differentiate tillage systems (Blanco-Canqui and Lal, 2010; Six et al., 2000). In this study, lower dispersion constants (k_2) in the direct seeding further imply that reduced disturbance not only preserves larger aggregates but may also increase their resistance to applied energy across all size fractions. We note, however, that our experiment was not designed to isolate the individual contributions of SOC inputs versus mechanical disturbance, and the mechanistic role of each factor should therefore be regarded as inferred from existing measurements and literature rather than experimentally confirmed here.

These results suggest that k_1/k_2 ratios and E_{crit} values may be

Table 4
Model parameters summary for soil dispersion characteristic curves (SDCCs) and aggregate liberation and dispersion curves (ALDCs).

Characteristic curves	A0 (%)	k1 (mL/J)	k2	Ecrit (J/mL)	Ratio k1/k2[a]	R^2
Luvisol (direct seeding)						
SDCC	23.90	-	0.027	-	-	
ALDC						
2–250 µm		0.270		9.4	9.8	0.99
2–53 µm		0.129		15.3	4.7	0.99
2–20 µm		0.115		16.3	4.2	0.92
2–6.3 µm		0.056		24.9	2.0	0.99
Luvisol (conventional tillage)						
SDCC	28.23	-	0.044	-	-	
ALDC						
2–250 µm		0.309		7.4	7.1	0.99
2–53 µm		0.245		8.6	5.6	0.98
2–20 µm		0.175		10.6	4.0	0.99
2–6.3 µm		0.106		14.3	2.4	0.90
Calcaric Regosol (24 years reclamation site)						
SDCC	20.27	-	0.032	-	-	
ALDC						
2–250 µm		0.454		6.3	14.2	0.99
2–53 µm		0.100		16.7	3.1	0.99
2–20 µm		0.057		23.1	1.8	0.99
2–6.3 µm		0.040		27.7	1.3	0.99
Luvisol (at mining area)						
SDCC	16.36	-	0.026	-	-	
ALDC						
2–250 µm		0.232		10.7	9.0	0.99
2–53 µm		0.151		14.1	5.9	0.99
2–20 µm		0.079		21.1	3.1	0.99
2–6.3 µm		0.043		29.7	1.7	0.99
Ferralsol						
SDCC	57.09	-	0.002	-	-	
ALDC						
2–250 µm		0.004		329.0	2.0	0.99
2–53 µm		0.003		405.2	1.4	0.99
2–20 µm		0.003		414.5	1.3	0.99
2–6.3 µm		0.002		459.0	1.1	0.99
Andosol						
SDCC	35.23	-	0.001	-	-	
ALDC						
2–250 µm		0.056		64.9	33.3	0.99
2–53 µm		0.002		514.3	1.3	0.99
2–20 µm		0.002		597.4	1.0	0.91
2–6.3 µm		0.001		655.5	0.8	0.99
Phaeozem						
SDCC	46.74	-	0.0006	-	-	
ALDC						
2–250 µm		0.0004		2146.1	0.6	0.26
2–53 µm		0.0003		2288.4	0.5	0.26
2–20 µm		0.0016		983.4	2.8	0.89
2–6.3 µm		0.0032		651.9	5.5	0.93

[a] For each soil, the k_2 value derived from the SDCC was used to calculate the k_1/k_2 ratio for all ALDC size fractions.

potentially useful for differentiating land management systems and could be developed as indices for comparative aggregate structural status, but further validation is needed before implementation. This interpretation is in line with recent energy-based SOC fractionation work showing that conservation systems express clearer management signals in intact macroaggregate fractions at low ultrasonic energy, whereas higher energies resolve more mineral-associated SOC pools linked to climate mitigation functions (Wieser et al., 2026). Together, such results support the broader use of energy-resolved fractionation to capture both management-sensitive aggregate structure and functionally distinct carbon pools. In comparison with classic aggregate stability tests based on single energy levels, our approach therefore provides an explicit, quantitative link between management practices, hierarchical fragmentation, and energy thresholds for aggregate disruption.

The mining-area soils showed different hierarchy and EcritEcrit patterns from the long-term managed Luvisols, although these differences also reflect contrasts in parent material, soil development, and reclamation history (Table 3, Fig. 3). The Calcaric Regosol, developed on Loess parent material, reflects the inherently fragile structure characteristic of Loess, which is particularly susceptible to rapid aggregate breakdown under water-induced disruption (Pihlap et al., 2021). Carbonate cementation ($CaCO_3$) in these soils is susceptible to dissolution, weakening aggregate cohesion and accelerating structural degradation (Pésci, 1990). The distinct aggregate hierarchy and greater susceptibility to dispersion observed in the reclaimed Calcaric Regosol, relative to the reference Luvisol, indicate that the development of complex aggregate organization remains influenced by both time since reclamation and soil organic carbon accumulation (Dexter et al., 2008; Lal, 2015; Pihlap et al., 2021). These findings suggest that hierarchy parameters could serve as useful indicators for assessing the structural development of reclaimed soils, although further validation across a wider range of reclamation systems is still required.

Taken together, these results advance the concept of aggregate hierarchy by demonstrating that contrasting pedogenic environments, characterized by distinct mineralogical and organic binding agents, exhibit different patterns of soil aggregation, resulting in measurable differences in aggregate resistance to disruption that are sensitive to land management. Differences among size fractions are consistent with the conceptual framework proposed by Tisdall and Oades (1982), suggesting that macroaggregation is strongly influenced by soil organic carbon and transient binding agents, whereas microaggregation appears more closely linked to more persistent, pedogenetically derived binding agents. However, our data do not provide direct proof of the relative contributions of individual binding agents (e.g. $CaCO_3$, SOC quality, clay mineralogy) within each size class, and this mechanistic interpretation should therefore be viewed as a hypothesis supported by known mechanisms and our energy-resolved patterns, rather than a definitive causal attribution.

The direct measurement of k_1/k_2 and E_{crit} across soils and size classes, and the demonstration of their responsiveness to mineralogical constitution and land management, establish that these parameters could be used as operational indicators of aggregate resistance and structural resilience. Moreover, these indices enable refined distinctions among soil types, management practices, and reclamation efforts, offering a practical means of assessing soil structural state. Recent work using a two-energy, two-size SOC fractionation scheme (0 and 60 J mL^{-1}; >50 and <50 μm) has likewise shown that energy-resolved size fractions can jointly characterize management-sensitive aggregate pools and more stable mineral-associated carbon, providing a framework for soil ecosystem health monitoring (Wieser et al., 2026). Integrating such SOC-focused approaches with hierarchy-based indices like k_1/k_2 and E_{crit} could, in future studies, support more comprehensive assessments of both structural resilience and biogeochemical functioning. Nevertheless, critical gaps remain, particularly regarding the temporal dynamics of these indicators, their sensitivity to complex field conditions, and their broader predictive power across diverse ecosystems and management regimes. Accordingly, the primary contribution of the present study is to provide quantitative, cross-system patterns in k_1/k_2 and E_{crit} that are consistent with known effects of SOC and carbonates on aggregation, and that can guide more detailed mechanistic work. Future research should aim to bridge these gaps, improving our capacity to monitor and manage soil aggregation and structural integrity for sustainable land use and ecosystem health.

5. Conclusion

The model employed, which quantifies the liberation and subsequent dispersion of soil aggregates across a range of size fractions and energies, effectively simulated aggregate breakdown in Ferralsols, Luvisols, Andosols, and Calcaric Regosols. However, it was less successful in explaining the behavior of the Phaeozem, highlighting limitations where carbonate-rich, C-rich systems display more complex dispersion behavior. Across all soils except the Phaeozem, the energy required to disrupt aggregates generally increased with aggregate size, supporting the concept of aggregate hierarchy and enabling quantitative comparison of fraction-specific behaviors.

Consistent with hierarchical theory, Luvisols exhibited pronounced, stepwise breakdown indicative of stronger hierarchy than Ferralsols and Andosols, while reclaimed soils displayed intermediate hierarchical organization.

Our findings further suggest that aggregate hierarchy can be modulated by soil management, extending previous views that considered hierarchy primarily as a mineralogically defined soil property. The study indicates that hierarchy may instead be a continuous characteristic influenced by organic matter inputs and disturbance history, reflecting a gradient rather than a binary trait. Therefore, the k_1/k_2 and E_{crit} indices should be interpreted as relative descriptors and are most meaningful for comparing different management systems within the same soil.

Finally, the modelling approach applied here provides a quantitative framework for evaluating this hierarchy gradient, moving beyond simplistic stable/unstable classifications toward a more nuanced understanding. Future research is needed to link these modeled hierarchy indices with direct characterization of binding agents and to test their robustness across diverse soils and management histories.

CRediT authorship contribution statement

Rodrigo Lima da Motta Junior: Writing – review & editing, Writing – original draft, Visualization, Methodology, Investigation, Formal analysis, Data curation, Conceptualization. **Steffen A. Schweizer:** Writing – review & editing, Visualization, Supervision, Methodology, Investigation, Conceptualization. **Bernardo Amorim da Silva:** Writing – review & editing, Visualization. **Franziska Bucka:** Writing – review & editing, Visualization, Formal analysis, Conceptualization. **Thiago M. Inagaki:** Writing – review & editing, Visualization, Formal analysis. **Noelia Garcia-Franco:** Writing – review & editing, Visualization, Formal analysis. **Evelin Pihlap:** Writing – review & editing, Visualization, Formal analysis. **Edson Marcio Mattiello:** Writing – review & editing. **Ingrid Kögel-Knabner:** Writing – review & editing, Conceptualization. **Pedro P. de C. Teixeira:** Writing – review & editing, Visualization, Supervision, Methodology, Investigation, Formal analysis, Conceptualization.

Declaration of Competing Interest

The authors declare that they have no known competing financial interests or personal relationships that could have appeared to influence the work reported in this paper.

Acknowledgments

We thank Martin Wiesmeier from the Bavarian State Research Center

for Agriculture (LfL) as well as Ulrich Doerfel from the Bavarian State Farms (BaySG) for support of the field sampling in Puch (Germany). We would like to acknowledge the Bayerisches Hochschulzentrum für Lateinamerika (BAYLAT) for the financial support for this study. We thank the contribution of the Technical University of Munich, soil department staff and technicians, especially Maria Greiner and Gertraud Harrington, for all the support. The authors acknowledge the Coordenação de Aperfeiçoamento de Pessoal de Nível Superior (CAPES, Brazil) for covering the Open Access publication fee through the CAPES–Elsevier Read and Publish agreement.

Data availability

Data will be made available on request.

References

Asano, M., Wagai, R., 2014. Evidence of aggregate hierarchy at micro- to submicron scales in an allophanic andisol. Geoderma 216, 62–74. https://doi.org/10.1016/j.geoderma.2013.10.005.

Blanco-Canqui, H., Lal, R., 2010. Principles of Soil Conservation and Management. Springer. https://doi.org/10.1007/978-1-4020-8709-7.

Breure, M.S., van der Sluijs, A.J., Koorneef, G.J., Salonen, A.-R., Pulleman, M.M., Hagens, M., Schenkeveld, W.D.C., Lonardo, D.P.Di, 2026. Glued forever: incomplete dispersion hampers POM-MAOM fractionation in soils with high SOC and metal (hydr)oxide content. Geoderma 467, 117704. https://doi.org/10.1016/j.geoderma.2026.117704.

Bronick, C.J., Lal, R., 2005. Soil structure and management: a review. Geoderma 124, 3–22. https://doi.org/10.1016/j.geoderma.2004.03.005.

Chenu, C., Plante, A.T., 2006. Clay-sized organo-mineral complexes in a cultivation chronosequence: revisiting the concept of the "primary organo-mineral complex. Eur. J. Soil. Sci. 57, 596–607. https://doi.org/10.1111/j.1365-2389.2006.00834.x.

Christensen, B.T., 2001. Physical fractionation of soil and structural and functional complexity in organic matter turnover. Eur. J. Soil. Sci. 52, 345–353. https://doi.org/10.1046/j.1365-2389.2001.00417.x.

Denef, K., Six, J., Merckx, R., Paustian, K., 2002. Short-term effects of biological and physical forces on aggregate formation in soils with different clay mineralogy. Plant. Soil. 246, 185–200. https://doi.org/10.1023/A:1020668013524.

Dexter, A.R., Richard, G., Arrouays, D., Czyz, E.A., Jolivet, C., Duval, O., 2008. Complexed organic matter controls soil physical properties. Geoderma 144, 620–627. https://doi.org/10.1016/j.geoderma.2008.01.022.

Emerson, W.W., Greenland, D.J., 1990. Soil aggregates — formation and stability. In: De Boodt, M., Hayes, M.H., Herbillon, A., De Strooper, E.B., Tuck, J. (Eds.), Soil Colloids and Their Associations in Aggregates. Springer, Boston, pp. 485–511. https://doi.org/10.1007/978-1-4899-2611-1_18.

Fatichi, S., Or, D., Walko, R., Vereecken, H., Young, M.H., Ghezzehei, T.A., Hengl, T., Kollet, S., Agam, N., Avissar, R., 2020. Soil structure is an important omission in earth system models. Nat. Commun. 11, 522. https://doi.org/10.1038/s41467-020-14411-z.

Field, D.J., Minasny, B., 1999. A description of aggregate liberation and dispersion in A horizons of Australian vertisols by ultrasonic agitation. Geoderma 91, 11–26. https://doi.org/10.1016/S0016-7061(98)00142-6.

Field, D.J., Minasny, B., Gaggin, M., 2006. Modelling aggregate liberation and dispersion of three soil types exposed to ultrasonic agitation. Aust. J. Soil. Res. 44, 497–502. https://doi.org/10.1071/SR05127.

Garcia-Franco, N., Walter, R., Wiesmeier, M., Hurtarte, L.C.C., Berauer, B.J., Buness, V., Zistl-Schlingmann, M., Kiese, R., Dannenmann, M., Kögel-Knabner, I., 2021. Biotic and abiotic controls on carbon storage in aggregates in calcareous alpine and prealpine grassland soils. Biol. Fertil. Soils 57, 203–218. https://doi.org/10.1007/s00374-021-01582-0.

Gee, G.W., Or, D., 2002. Particle-size analysis. In: Dane, J.H., Topp, G.C. (Eds.), Methods of Soil Analysis. Soil Science Society of America, pp. 255–293. https://doi.org/10.2136/sssabookser5.4.c12.

Inagaki, T.M., Possinger, A.R., Grant, K.E., Schweizer, S.A., Mueller, C.W., Derry, L.A., Lehmann, J., Kögel-Knabner, I., 2020. Subsoil organo-mineral associations under contrasting climate conditions. Geochim. Cosmochim. Acta 270, 244–263. https://doi.org/10.1016/j.gca.2019.11.030.

IUSS Working Group, W.R.B., 2015. World reference base for soil resources 2014. The International Soil Classification System WRB, Third Edition, 2014. Springer Water.

Jarvis, S., Tisdall, J., Oades, M., Six, J., Gregorich, E., Kögel-Knabner, I., 2012. Landmark papers. Eur. J. Soil. Sci. 63, 1–21. https://doi.org/10.1111/j.1365-2389.2011.01408.x.

Kögel-Knabner, I., Amelung, W., 2021. Soil organic matter in major pedogenic soil groups. Geoderma 384, 114785. https://doi.org/10.1016/j.geoderma.2020.114785.

Krauss, M., Wiesmeier, M., Don, A., Cuperus, F., Gattinger, A., Gruber, S., Haagsma, W. K., Peigné, J., Palazzoli, M.C., Schulz, F., van der Heijden, M.G.A., Vincent-Caboud, L., Wittwer, R.A., Zikeli, S., Steffens, M., 2022. Reduced tillage in organic farming affects soil organic carbon stocks in temperate Europe. Soil. Tillage Res. 216, 105262. https://doi.org/10.1016/j.still.2021.105262.

Lal, R., 2015. Restoring soil quality to mitigate soil degradation. Sustainability 7, 5875–5895. https://doi.org/10.3390/su7055875.

North, P.F., 1976. Towards an absolute measurement of soil structural stability using ultrasound. J. Soil. Sci. 27, 451–459. https://doi.org/10.1111/j.1365-2389.1976.tb02014.x.

Oades, J.M., 1984. Soil organic matter and structural stability: mechanisms and implications for management. Plant. Soil. 76, 319–337. https://doi.org/10.1007/BF02205590.

Oades, J.M., 1989. An introduction to organic matter in mineral soils. In: Dixon, J., Weed, S. (Eds.), Minerals in Soil Environments, pp. 89–159. https://doi.org/10.2136/sssabookser1.2ed.c3.

Oades, J.M., Waters, A.G., 1991. Aggregate hierarchy in soils. Aust. J. Soil. Res. 29, 815–825. https://doi.org/10.1071/SR9910815.

Pésci, M., 1990. Loess is not just the accumulation of dust. Quat. Int. 7 (8), 1–21.

Pihlap, E., Steffens, M., Kögel-Knabner, I., 2021. Initial soil aggregate formation and stabilisation in soils developed from calcareous loess. Geoderma 385, 114854. https://doi.org/10.1016/j.geoderma.2020.114854.

Poeplau, C., Sigurdsson, P., Sigurdsson, B.D., 2020. Depletion of soil carbon and aggregation after strong warming of a subarctic Andosol under forest and grassland cover. Soil 6, 115–129. https://doi.org/10.5194/soil-6-115-2020.

R Core Team, 2026. R: a language and environment for statistical computing. R Found. Stat. Comput. https://doi.org/10.4236/oalib.1107821.

Six, J., Bossuyt, H., Degryze, S., Denef, K., 2004. A history of research on the link between (micro)aggregates, soil biota, and soil organic matter dynamics. Soil. Tillage Res. 79, 7–31. https://doi.org/10.1016/j.still.2004.03.008.

Six, J., Elliott, E., Paustian, K., 2000. Soil macroaggregate turnover and microaggregate formation: a mechanism for C sequestration under no-tillage agriculture. Soil. Biol. Biochem. 32, 2099–2103. https://doi.org/10.1016/S0038-0717(00)00179-6.

Teixeira, P.P.C., Vidal, A., Teixeira, A.P.M., Souza, I.F., Hurtarte, L.C.C., Silva, D.H.S., Almeida, L.F.J., Buegger, F., Hammer, E.C., Jansa, J., Mueller, C.W., Silva, I.R., 2024. Decoding the rhizodeposit-derived carbon's journey into soil organic matter. Geoderma 443, 116811. https://doi.org/10.1016/j.geoderma.2024.116811.

Tisdall, J.M., Oades, J.M., 1982. Organic matter and water-stable aggregates in soils. J. Soil. Sci. 33, 141–163. https://doi.org/10.1111/j.1365-2389.1982.tb01755.x.

Totsche, K.U., Amelung, W., Gerzabek, M.H., Guggenberger, G., Klumpp, E., Knief, C., Lehndorff, E., Mikutta, R., Peth, S., Prechtel, A., Ray, N., Kögel-Knabner, I., 2018. Microaggregates in soils. J. Plant. Nutr. Soil. Sci. 181, 104–136. https://doi.org/10.1002/jpln.201600451.

Vrdoljak, G., Sposito, G., 2002. Soil aggregate hierarchy in a Brazilian oxisol. Dev. Soil. Sci. 28, 197–217. https://doi.org/10.1016/S0166-2481(02)80054-X.

Wieser, S., Keiblinger, K., Mayer, H., Rosinger, C., Mentler, A., Wriessnig, K., Bruhn, N., Schott, K., Ploszczanski, L., Hood-Nowotny, R., Bodner, G., 2026. Energy matters: soil organic carbon fractions as soil health indicator or characterizing ecosystem property. Soil. Tillage Res. 257, 106927. https://doi.org/10.1016/j.still.2025.106927.

Wu, T., Ost, A.D., Audinot, J.N., Wiesmeier, M., Wirtz, T., Buegger, F., Häusler, W., Höschen, C., Mueller, C.W., 2022. Association of fresh low-molecular-weight organic compounds with clay-sized mineral fraction in soils of different organic carbon loading. Geoderma 409, 115657. https://doi.org/10.1016/j.geoderma.2021.115657.